An Improved ISUM Rectangular Plate Element†

—Taking Account of Post-Ultimate Strength Behavior—

Yukio UEDA*, Sherif M.H. RASHED** and Yehia ABDEL-NASSER***

Abstract

In the framework of the Idealized Structural Unit Method (ISUM), a rectangular plate element has been developed. This element takes accout of bukling, post-buckling behavior and ultimate strength of the plate. After ultimate strength, the element predicts a constant carrying capacity in contrast with the decreasing carrying capacity of actual plates after they reach their ultimate strength.

In the ultimate strength analysis of redundant structures, such as ships, highly loaded plate panels may reach their ultimate strength and exhibit considerable plastic deformation, thus losing a portion of their carrying capacity, before the whole structure reaches its ultimate strength.

In this paper, an improved element is presented in which the effectiveness of the plate after buckling is expressed as a function of the total strain, and a new concept of strain hardening is introduced in evaluating the post-ultimate strength elastic-plastic stiffness matrix. In this way, after the element reaches its ultimate strength the reduction of plate strength with the increase of inplane displacement can be evaluated. Comparison of results of analysis by this improved element with those by the Finite Element Method indicates good accuracy of the new element in practical use.

KEY WORDS: (Rectangular Plate) (ISUM) (Buckling) (Ultimate Strenbth) (Post-Ultimate Strength) (In-Plane Rigidity)

1. Introduction

In the late ninteen sixties to early seventies. Ueda and Rashed[1] developed an effective method of analysis of non-linear behavior of large structures. In 1975[2], the method was called "The Idealized Structural Unit Method". In this method, the structure is divided into the biggest possible structural units(components), whose geometric and material nonlinear behavior are idealized. These structural units are regarded as elements in the framework of the matrix displacement method of stractural analysis.

In the middle eighties[3,4], a rectangular plate element and a rectangular stiffened plate element have been developed. The developed elements predict the behavior until their ultimate strength with an accuracy simillar to those of other accepted theoretical methods. These elements, however, predict a constant post-ultimate strength. The reason for this is that the effectiveness of the plate panels is expressed in terms of maximum stress in the elastic as well as the elastic-plastic ranges. After yielding, the maximum stress does not change leading to a constant effectiveness and a constant carrying capcity.

Actual plate panels exhibit post-yield reduction of effectiveness with the increase of inplane displacements, that is with increasing strain.

In this paper a further development of the ISUM rectangular plate element has been carried out to include this effect. An improved element is presented in which the post-buckling stiffness matrix is expressed as a function of the total strain and a new concept of strain hardening is introduced in evaluating the post-ultimate strength elastic-plastic stiffness matrix.

In this way, the reduction of plate strength with increased in-plane displacement after yielding may be evaluated.

Several examples of rectangular plates with different thicnesses subjected to in-plane uniaxial compression, biaxial compression and shearing loads are presented and compared with results of analysis by the Finite Element Method.

2. Perfect Rectangular Plate Element

Each ship plate panel, unavoidably, has a certain amount of initial deflection and residual stresses caused by

† Received on May 6, 1992

* Director, professor
** Technical Manager, MSC Japan Ltd.
*** Graduate Student Osaka University

Transactions of JWRI is published by Welding Research Institute of Osaka University, Ibaraki, Osaka 567, Japan

fabrication processes. First a perfect flat rectangular plate element free from initial deflection and residual stresses is considered. The effect of these initial imperfections is considered in the next section.

Following procedures presented by Ueda et. el[3], the plate element has only four nodal points with two degrees of freedom at each nodal point as shown in **Fig. 1**. The nodal displacement and the nodal force vectors are presented as follows.

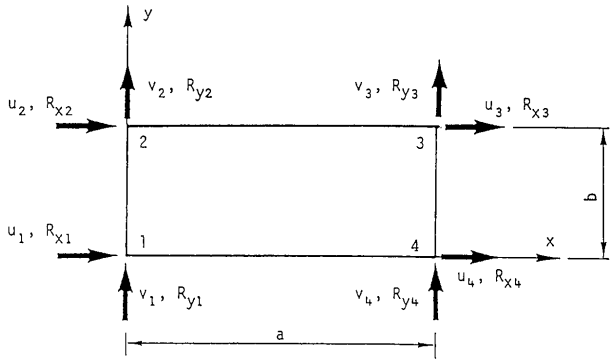

Fig. 1 ISUM rectangular plate element

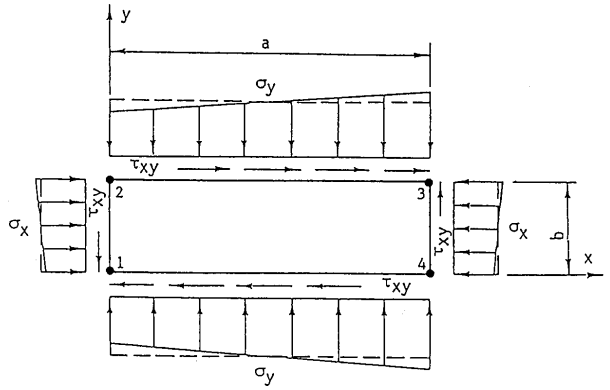

Fig. 2 ISUM element and applied loads

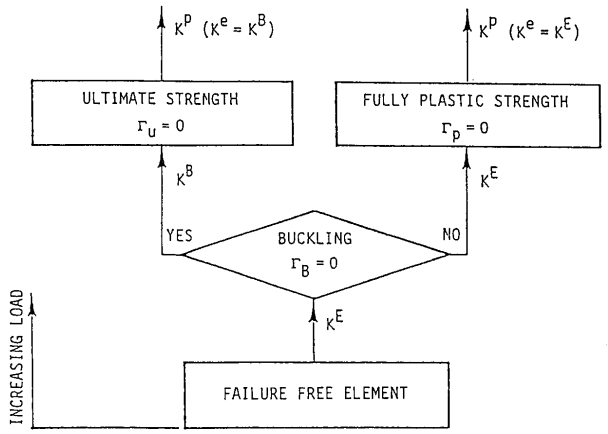

Fig. 3 Behavior of the rectangular plate element

$$U = [U_1\ U_2\ U_3\ U_4]^T,\ U_i = [u_i, v_i]^T \tag{1}$$

$$R = [R_1\ R_2\ R_3\ R_4]^T,\ R_i = [R_{xi},\ R_{yi}]^T \tag{2}$$

where, a suffix T indicates the transposed matrix.

The plate is simply supported at its edges. In-plane biaxial compressive force, in-plane bending moments and in-plane shearing forces are applied as shown in **Fig. 2**.

2.1 General behavior of the rectangular plate element

The behavior of the rectangular plate element when subjected to an increasing load is illustrated in **Fig. 3** and may be summarized as follows:

The relation between the nodal force vector **R** and the nodal displacement vector **U** may be conveniently expressed in the incremental form. Before any failures have taken place, the relation between an increment $\Delta\mathbf{R}$ of the nodal force vector R and an increment $\Delta\mathbf{U}$ of the nodal displacement vector **U** may be expressed in terms of an elastic stiffness matrix K^E as follows.

$$\Delta \boldsymbol{R} = K^E \Delta \boldsymbol{U} \tag{3}$$

As the nodal forces increase, the plate may buckle when a buckling condition is satisfied.

$$\Gamma_B = 0 \tag{4}$$

where, Γ_B is a buckling function.

After buckling, the relation between $\Delta\mathbf{R}$ and $\Delta\mathbf{U}$ may be expressed in terms of a tangential stiffness matrix K^B, taking account of post-buckling effects, as follows.

$$\Delta \boldsymbol{R} = K^B \Delta \boldsymbol{U} \tag{5}$$

The element may continue to carry further load until yielding starts and spreads over a sufficient area of the element. This causes the element to reach its ultimate strength. A condition for yielding. Γ_{yi} at any point i may be written as follows.

$$\Gamma_{yi} = 0 \tag{6}$$

After yielding starts, the relation between $\Delta\boldsymbol{R}$ and $\Delta\boldsymbol{U}$ may be expressed in terms of an elastic-plastic stiffness matrix K^P with the aid of the plastic node method as follows.

$$\Delta \boldsymbol{R} = K^P \Delta \boldsymbol{U} \tag{7}$$

K^E, Γ_B and Γ_{yi} appearing in Eqs. (3) to (6) are similar to those in Ref. 3) and are summarized in the following

sections for completion of presentation. K^B will rewritten in terms of strain, ε and K^P is newly derived on the base of a new concept to account for post-ultimate strength behavior.

If the properties of the element are such that buckling does not occur until the element reaches its fully plastic strength, the yield condition and $\Delta \boldsymbol{R}$-$\Delta \boldsymbol{U}$ relationship in the the post-fully-plastic strength state may be expressed similarly by Eqs. (6) and (7).

Expressions for Γ_{yi} and K^P in this case may be found in Ref. 3).

2.2 Failure-free stiffness matrix

Before any local failure, such as buckling, of the plate element occurs displacement functions satisfying the conditions of linearly varying boundary displacement and constant shear strain along the plate sides are assumed as follows.

$$\left.\begin{aligned} u &= a_1 + a_2 x + a_3 y + a_4 xy + b_4(b^2 - y^2)/2 \\ v &= b_1 + b_2 x + b_3 y + b_4 xy + a_4(a^2 - x^2)/2 \end{aligned}\right\} \quad (8)$$

where,

u and v are the displacements in x and y directions at a point $(x.y)$,

i_1 and i_1 are coefficients, and,

a and b are the length and breadth of the element.

Following the procedures of the Finite Element Method, the relation between $\Delta\varepsilon$, an increment of the the strain vector ε to $\Delta \boldsymbol{U}$, an increment of the nodal displacement vector $\boldsymbol{U}$ may be derived as follows.

$$\Delta\varepsilon = B\Delta U \quad (9)$$

where, $\Delta\varepsilon = [\Delta\varepsilon_x \ \Delta\varepsilon_y \ \Delta\varepsilon_{xy}]^T$ and

B is the strain-displacement matrix

The relation between $\Delta\sigma$, an increment of the stress vector σ and $\Delta\varepsilon$ may be written as follows.

$$\Delta\sigma = D^E \ \Delta\varepsilon \quad (10)$$

where, $\Delta\sigma = [\Delta\sigma_x \ \Delta\sigma_y \ \Delta\tau_{xy}]^T$ and,

D^E is the stress-strain matrix in the elastic range.

$$D^E = \frac{E}{1-\nu^2}\begin{bmatrix} 1 & \nu & 0 \\ \nu & 1 & 0 \\ 0 & 0 & (1-\nu)/2 \end{bmatrix}$$

The elastic failure free stiffness matrix K^E may then be derived as follows.

$$K^E = \int_v B^T D^E B \, dv \quad (11)$$

where v is the volume of the element.

The stress in the element may be expressed as

$$\sigma = D^E \varepsilon = D^E B U$$

2.3 Buckling Condition Γ_B

In ship structures, considerable in-plane bending moments may act on large stiffened plate structures such as decks, sides or bottom plating. Considering only one plate panel out of such a large construction, in-plane bending moment acting on such a plate panel is small and may be neglected when checking buckling in terms of average stresses.

Based on an analytical-numerical solution[3], the buckling condition. Γ_B, of the rectangular plate element may then be written in terms of average normal stresses σ_{xav} in x direction and σ_{yav} in y direction and a uniform shearing stress τ_{xy} as follows,

1- when σ_{xav} is tension and σ_{yav} is compression ($\sigma_{xav} < 0, \sigma_{yav} > 0$)

$$\Gamma_B = \frac{(m^2+\beta^2)^2 \ \sigma_{xav}}{m^2(1+\beta^2)^2\sigma_{xcr}} + \frac{\sigma_{yav}}{\sigma_{ycr}} + \left(\frac{\tau_{xy}}{\tau_{xycr}}\right)^2 - 1 \quad (12.a)$$

2- when σ_{xav} is compression and σ_{yav} is tension ($\sigma_{xav} > 0, \sigma_{yav} < 0$)

$$\Gamma_B = \frac{(1+\beta^2)^2 \ \sigma_{yav}}{(m^2+\beta^2)^2\sigma_{ycr}} + \frac{\sigma_{xav}}{\sigma_{xcr}} + \left(\frac{\tau_{xy}}{\tau_{xycr}}\right)^2 - 1 \quad (12.b)$$

3- when σ_{xav} is compression and σ_{yav} is compression ($\sigma_{xav} > 0, \sigma_{yav} > 0$)

$$\Gamma_B = \left[\frac{(\sigma_{xav}/\sigma_{xcr})}{1-(\tau_{xy}/\tau_{xycr})^2}\right]^{\alpha_1} + \left[\frac{(\sigma_{yav}/\sigma_{ycr})}{1-(\tau_{xy}/\tau_{xycr})^2}\right]^{\alpha_2} - 1 \quad (12.c)$$

where, σ_{xcr}, σ_{ycr} and τ_{xycr} are the buckling stresses when each stress acts alone on the plate, m is the number of half waves of buckling when the plate buckles under the action of σ_{xav} alone.

β = a/b: aspect ratio of the plate,

$\alpha_1 = \alpha_2 = 1$ For $1/\sqrt{2} \leqq \beta \leqq \sqrt{2}$, and,

$$\left.\begin{aligned} \alpha_1 &= 0.0293\beta^3 - 0.3364\beta^2 + 1.584\beta - 1.0596 \\ \alpha_2 &= 0.0049\beta^3 - 0.1183\beta^2 + 0.515\beta + 0.8522 \end{aligned}\right\}$$

For $\beta > \sqrt{2}$

When Γ_B is smaller than zero, it indicates that the plate

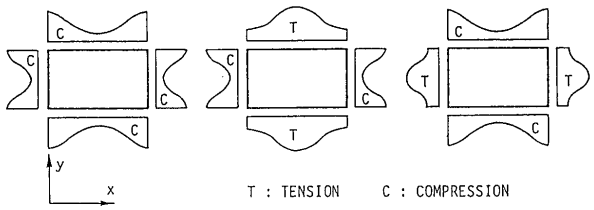

Fig. 4 Stress distribution in a buckled plate.

has not buckled. When Γ_B is greater than or equal to zero, it indicates that the plate has buckled.

2.4 Post-buckling behavior and stiffness matrix

After the plate element has buckled, out-of-plane deflection is induced and the stress distribution in the middle plane of the element (membrane stress) becomes nonlinear. In order to continue to use the same displacement functions as Eq. (8) in the post buckling range, an imaginary flat plate with linear stress distribution is considered. The material properties of this imaginary plate are determined such that it shows overall deformation equal to that of the buckled plate under the same load (same stiffness). First let us consider a plate element which has buckled under in-plane biaxial compressive and shearing forces. The stress distribution in the middle plane of the plate is as shown in **Fig. 4** . The shortenings δ_x and δ_y in x and y directions and the shear strain γ_{xyav} of the buckled plate may be evaluated as follows,

$$\left.\begin{aligned}
\delta_x &= a\varepsilon_{xav} = \int_0^a \varepsilon_x)_{y=0}dx = \int_0^a [(\sigma_x/E)_{y=0} - \nu\sigma_y/E)_{y=0}]\,dx \\
&= a(\sigma_{xmax} - \nu\sigma_{yav})/E \\
\delta_y &= b\varepsilon_{yav} = \int_0^b \varepsilon_y)_{x=0}\,dy = \int_0^b [(\sigma_y/E)_{x=0} - \nu\sigma_x/E)_{x=0}]\,dy \\
&= b(\sigma_{ymax} - \nu\sigma_{xav})/E \\
\gamma_{xyav} &= \tau_{xy}/G_e
\end{aligned}\right\} \tag{13}$$

where σ_{xmax} and σ_{ymax} are the maximum stresses in x and y directions. They may be expressed as follows[3].

$$\left.\begin{aligned}
\sigma_{xmax} &= f_1 + f_2\ \sigma_{xav} + (f_3+\nu)\sigma_{yav} + f_4 \\
\sigma_{ymax} &= g_1 + (g_2+\nu)\sigma_{xav} + g_3\sigma_{yav} + g_4
\end{aligned}\right\} \tag{14}$$

where,

$f_1 = 1.62\sigma_{xcr}\nu^{2.4}$ $\quad f_2 = (f_v+1)\xi_1 + 1$

$f_3 = (f_v+1)\xi_2 - \nu$ $\quad f_4 = -(f_v+1)\xi_3\pi^2m^2D/ta^2$

$g_1 = 1.62\sigma_{ycr}\nu^{2.4}$ $\quad g_2 = (g_v+1)\xi_2 - \nu$

$g_3 = (g_v+1)\xi_1(a^4/m^4b^4) + 1$ $\quad g_4 = -(g_v+1)\xi_3\pi^2D/tb^2$

and,

$$\xi_1 = \frac{2m^4b^4}{a^4+m^4b^4},\quad \xi_2 = \frac{2m^2a^2b^2}{a^4+m^4b^4},\quad \xi_3 = \frac{2(a^2+m^2b^2)^2}{a^4+m^4b^4}$$

$D = Et^3/12/(1-\nu^2)$

$\nu = |\ \tau_{xy}\ |\ /\tau_{xycr}$

$f_v = 0.62\nu$ $\quad \alpha_{xmax}{}^* \leqq 0$

$f_v = 1.3\nu^{1.5}$ $\quad \alpha_{xmax}{}^* > 0,\ \nu \leqq 1$

$f_v = 1.3\nu$ $\quad \alpha_{xmax}{}^* > 0,\ \nu > 1$

$g_v = 0.62\nu$ $\quad \alpha_{ymax}{}^* \leqq 0$

$g_v = 1.3\nu^{1.5}$ $\quad \alpha_{ymax}{}^* > 0,\ \nu \leqq 1$

$g_v = 1.3\nu$ $\quad \alpha_{ymax}{}^* > 0,\ \nu \leqq 1$

and,

$$\alpha_{xmax}{}^* = \xi_1 + \xi_2(\sigma_{yav}/\sigma_{xav}) - (\pi^2m^2D/a^2)\xi_3/(\sigma_{xav}t)$$

$$\alpha_{ymax}{}^* = \xi_2\sigma_{xav}/\sigma_{yav} + (a^4/m^4b^4)\xi_1 - (\pi^2D/b^2)/(\sigma_{yav}t)$$

and,

G_e = the effective shear modulus

$$= \frac{G}{C_2}\left(C_1\frac{\sigma_{xav}}{\sigma_{xcr}} + C_2\right)\left(C_1\frac{\sigma_{yav}}{\sigma_{ycr}} + C_2\right)$$

$$C_1 = \frac{12.915}{\nu-15} - \frac{5.166}{\nu+5} + 1.6482,\quad C_2 = \frac{8.4}{\nu+5} - 0.4$$

$$G = E/2/(1+\nu)$$

From Eq. (13), the relation between the average strain and the average stress may be written as follows.

$$\left.\begin{aligned}
\varepsilon_{xav} &= (\sigma_{xmax} - \nu\sigma_{yav})/E \\
\varepsilon_{yav} &= (-\nu\sigma_{xav} + \sigma_{ymax})/E \\
\gamma_{xy} &= \tau_{xy}/G_e
\end{aligned}\right\} \tag{15}$$

Substituting the maximum stresses σ_{xmax} and σ_{ymax} of Eq. (14) into Eq. (15), the relation between the average stress and the average strain may be rewritten as follows.

$$\left.\begin{aligned}
\sigma_{xav} &= \frac{1}{f_2g_3 - g_2f_3}\left(\left(Eg_3 + \frac{f_3(g_1+g_4) - g_3(f_1+f_4)}{\varepsilon_{xav}}\right)\varepsilon_{xav} - Ef_3\ \varepsilon_{yav}\right) \\
\sigma_{yav} &= \frac{1}{f_2g_3 - g_2f_3}\left(-Eg_2\varepsilon_{xav} + \left(Ef_2 + \frac{g_2(f_1+f_4) - f_2(g_1+g_4)}{\varepsilon_{yav}}\right)\varepsilon_{yav}\right) \\
\tau_{xy} &= G_e\ \gamma_{xy}
\end{aligned}\right\} \tag{16}$$

Now, the buckled plate is replaced by an imaginary flat plate of a homogeneous material. Then, the stress-strain relationship of Eq. (16) may be considered to be that of the material of the imaginary plate and written in the following form.

$$\sigma_{im} = D^{im}\varepsilon_{im} \tag{17}$$

where, D^{im} is the stress-strain ($\sigma_{im} - \varepsilon_{im}$) matrix of the imaginary plate and is give by

$$D^{im}=\frac{1}{E_1}\begin{pmatrix} Eg_3+\dfrac{f_3(g_1+g_4)-g_3(f_1+f_4)}{\varepsilon_{xim}} & -Ef_3 & 0 \\ -Eg_2 & Ef_2+\dfrac{g_2(f_1+f_4)-f_2(g_1+g_4)}{\varepsilon_{yim}} & 0 \\ 0 & 0 & E_1G_e \end{pmatrix}$$

where, $E_1=f_2g_3-g_2f_3$

It is to be noted here that D^{im} is derived for a combined load of biaxial compression and shear. This matrix can be applied, however, for combined loads of biaxial compression, biaxial in-plane bending and shear, since in-plane bending moments are small in plate panels and assumed to have small effect on the post-buckling stiffness.

Expressing Eq. (17) in an incremental form, $\Delta\sigma_{im}$, an increment of the stress σ_{im}, is expressed as follows.

$$\begin{aligned}\Delta\sigma_{im}&=D^{im}\Delta\varepsilon_{im}+\Delta D^{im}\varepsilon_{im} \qquad (18)\\ &=D^{im}\Delta\varepsilon_{im}+\frac{dD^{im}}{d\varepsilon_{im}}\Delta\varepsilon_{im}\varepsilon_{im}\\ \Delta\sigma_{im}&=D^{im}\Delta\varepsilon_{im}+\frac{\partial D^{im}}{\partial\varepsilon_{im}}\varepsilon_{im}\Delta\varepsilon_{im}+\frac{\partial D^{im}}{\partial\sigma_{im}}\varepsilon_{im}\frac{d\sigma_{im}}{d\varepsilon_{im}}\Delta\varepsilon_{im}\end{aligned}$$

from which

$$\Delta\sigma_{im}=D^{B}\ \Delta\varepsilon_{im} \qquad (19)$$

where, D^{B} = the relation between an increment of stress and an increment of strain of the imaginary plate, and is expressed as

$$D^{B}=(\mathrm{I}-\frac{\partial D^{im}}{\partial\sigma_{im}}\varepsilon_{im})^{-1}(D^{im}+\frac{\partial D^{im}}{\partial\varepsilon_{im}}\varepsilon_{im}) \qquad (20)$$

where, I=the unit matrix.

$$\frac{\partial D^{im}}{\partial\varepsilon_{im}}\varepsilon_{im}=[\frac{\partial D_{im}}{\partial\varepsilon_{xim}}\varepsilon_{im}\quad\frac{\partial D^{im}}{\partial\varepsilon_{yim}}\varepsilon_{im}\quad\frac{\partial D^{im}}{\partial\varepsilon_{xyim}}\varepsilon_{im}],$$

$$\frac{\partial D^{im}}{\partial\sigma_{im}}\varepsilon_{im}=[\frac{\partial D_{im}}{\partial\sigma_{xim}}\varepsilon_{im}\quad\frac{\partial D^{im}}{\partial\sigma_{yim}}\varepsilon_{im}\quad\frac{\partial D^{im}}{\partial\tau_{xyim}}\varepsilon_{im}]$$

The stiffness matrix K_{im} of the imaginary plate may be written as follows.

$$K^{B}_{im}=\int_v B^{T}D^{B}B\ dv \qquad (21)$$

where, B is the strain-displacement matrix derived from Eq. (8).

Recalling that the original buckled plate and the imaginary plate exhibit the same stiffness, the post buckling stiffness matrix K^{B} is given as follows.

$$K^{B}=K^{B}{}_{im}=\int_v B^{T}D^{B}B\ dv \qquad (22)$$

2.5 Plate behavior after yielding

For simplicity of presentation, let a rectangular plate simply supported along its four edges and subjected to uniaxial compression in the longitudinal direction be considered. After buckling, a stress distribution as shown in **Fig. 5** is developed in the middle plane of the plate. As the load increases yielding may start at points A and B where the membrane stress is maximam in compression (minimum) in x direction and maximum in tension (maximum) in y direction, or at the concave surface of the plate at center. The latter causes a decrease of bending stiffness leading to a higher rate of increase of deflection, and finally yielding at points A and B. As the plastic zone spreads around points A and B, the plate reaches its ultimate strength. As the plate continues to be compressed (imposed displacement), deflection increases causing a decrease of plate effective width. Meanwhile, shortening of edges *1-2* and *3-4* produces plastic strain sround points A and B. If the material is elastic perfectly plastic, the magnitude of σ_{xmax} (at the edges) does not show appreciable change. A decreasing effective breadth with constant σ_{xmax} leads to decrease the compressive force.

In this work, surface yielding is ignored and plasticity is assumed to be concentrated at points where yielding has started at the edges, according to the plastic node method.

2.6 Ultimate strength condition

As mentioned in the preceding sections, in the case of a simply supported rectangular plate element which has buckled under in-plane biaxial compression, in-plane bending and shear, the maximum membrane stresses are developed along the edges. Yielding starts at any one or combination of locations at the four corners or in the middle of each half buckling wave at the edges, see Fig. 5. Then, Yielding will be examined at these points which are called here checking points of plasticity.

σ_x at $y=0$, b, σ_y at $x=0$, a and τ_{xy} may be expressed in terms of nodal forces as follows.

$$\begin{aligned}&\sigma=S_1R\\ &S_1=D^{p1}BK^{-1}\end{aligned} \qquad (23)$$

In the above equation, D^{p1} defines the relationship of the maximum stresses to the average strains.

$$D^{p1}=E_e\begin{pmatrix} 1 & \nu a_e/a & 0 \\ \nu b_e/b & 1 & 0 \\ 0 & 0 & G_e/G_e \end{pmatrix}$$

where, $E_e=E/[1-(b_ea_e/ba)\nu^2]$ and, b_e and a_e are the effective widths of the plate element in x and y directions,

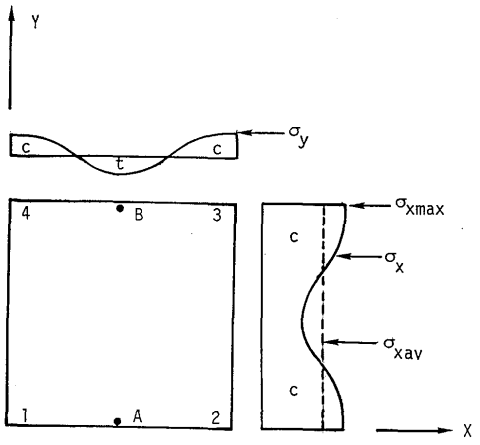

Fig. 5 Stress distribution after buckling under uniaxial compression

respectively.

$$b_e/b=\sigma_{xav}/\sigma_{xmax}=1/[1+f_1/\sigma_{xav})+(f_v+1)\alpha_{xmax}{}^*] \quad (24.a)$$

$$a_e/a=\sigma_{yav}/\sigma_{ymax}=1/[1+(g_1/\sigma_{yav})+(g_v+1)\alpha_{ymax}{}^*] \quad (24.b)$$

σ_x at $x=0$ and a, $y=b/2$ may be evaluated as follows,

$$\sigma_x=\sigma_{xav}(1-\alpha_{xmin})=D_1{}^{im}B\ K^{-1}R(1-\alpha_{xmin}) \quad (25)$$

where,

$$\alpha_{xmin}=1.3(\sigma_{xcr}/\sigma_{xav})v^{2.1}+\alpha_{xmin}{}^*(0.3v+1),$$

$$\alpha_{xmin}{}^*=\xi_1+\xi_2\frac{\sigma_{yav}}{\sigma_{xav}}-\frac{\pi^2m^2D}{a_4}\xi_3\frac{1}{\sigma_{xav}t},$$

and, $D_1{}^{im}$ is the first row of the matrix D^{im}.

σ_y at $y=0$, b in the middle of half buckling waves ($x=l/2$ where l is the length of one half buckling wave) may be evaluated as follows.

$$\sigma_y=\sigma_{yav}(1-\alpha_{ymin})=D_2{}^{im}B\ K^{-1}R(1-\alpha_{ymin}) \quad (26)$$

where,

$$\alpha_{ymin}=1.3(\sigma_{ycr}/\sigma_{yav})v^{2.1}+\alpha_{ymin}{}^*(0.3v+1),$$

$$\alpha_{ymin}{}^*=\xi_2\frac{\sigma_{xav}}{\sigma_{yav}}+\frac{a^4}{m^4b^4}\xi_1-\frac{\pi^2D}{b^2}\xi_3\frac{1}{\sigma_{yav}t},$$

and, $D_2{}^{im}$ is the second row of the matrix D^{im}.

Yielding is assumed to start at any of the checking points where the Mises yield condition is satisfied, that is

$$\Gamma_y=\sigma_x{}^2-\sigma_x\sigma_y+\sigma_y{}^2+3\tau_{xy}{}^2-\sigma_0{}^2=0 \quad (27)$$

Expressing stresses in terms of nodal forces, the yield condition may be written as follows.

$$\Gamma_y=\Gamma_y(R)=0 \quad (28)$$

Ultimate strength will be reached after yielding has occurred at a sufficient number of locations.

2.7 Stress strain relationship after yielding

After yielding has started at one or more locations, the following assumptions are made

1. the material is elastic-perfectly-plastic.

2. the total relative axial displacement, u along an edge where yielding has started may be divided into elastic component u^e and plastic component u^p

$$u=u^e+u^p \quad (29)$$

Dividing Eq. (29) by the length of an appropriate edge (a or b) the following expressions for average strains ε_{xav} and ε_{yav}

$$\left.\begin{aligned}\varepsilon_{xav}&=\varepsilon^e{}_{xav}+\varepsilon^p{}_{xav} \quad \text{at } y=0 \text{ or } b\\ \varepsilon_{yav}&=\varepsilon^e{}_{yav}+\varepsilon^p{}_{yav} \quad \text{at } x=0 \text{ or } a\end{aligned}\right\} \quad (30)$$

where superscripts e and p indicate elastic and plastic respectively.

3. The average shear strain γ_{xy} may be divided into elastic component $\gamma^e{}_{xy}$ and plastic component $\gamma^e{}_{xy}$

$$\gamma_{xy}=\gamma^e{}_{xy}+\gamma^p{}_{xy} \quad (31)$$

Equation (30) and (31) may be assumed as follows.

$$\{\varepsilon_{av}\}=\{\varepsilon^e{}_{av}\}+\{\varepsilon^p{}_{av}\} \quad (32)$$

Now let the imaginary plate appeared before be considered again. The strain $\{\varepsilon_{im}\}$ is equal to $\{\varepsilon_{av}\}$ and may be divided into elastic component $\varepsilon^e{}_{im}$ and plastic component $\varepsilon^p{}_{im}$

$$\varepsilon_{im}=\varepsilon^e{}_{im}+\varepsilon^p{}_{im} \quad (33)$$

Taking,

$$\left.\begin{aligned}&\varepsilon^e{}_{im}=\varepsilon^e{}_{av} \text{ and}\\ &\varepsilon^p{}_{im}=\varepsilon^p{}_{av},\end{aligned}\right\} \quad (34)$$

The following two assumptions are made.

4. The average stress σ_{av} is related to the elastic component of the average strain $\varepsilon^e{}_{av}$ by Eq. (16). That is σ_{im}, the

stress of the imaginary plate, is related to ε^{e}_{im}, the elastic component of the strain of the imaginary plate by the secant stress-strain matrix D^{im} of Eq. (17)

$$\sigma_{im}=D^{im}\ \varepsilon^{e}_{im} \tag{35}$$

5. The secant stress-strain matrix, D^{im} is assumed to be a function of the total strain, ε_{im}.

Now stress increment $\Delta\sigma_{im}$ caused by strain increment $\Delta\varepsilon_{im}$ may be calculated as follows.

A strain increment $\Delta\varepsilon_{im}$ causes stress increment $\Delta\sigma_{im}$ and an increment of D^{im}, ΔD^{im}. Taking account of these increments, Eq. (35) may be written as follows.

$$(\sigma_{im}+\Delta\sigma_{im})=(D^{im}+\Delta D^{im})+(\varepsilon^{e}_{im}+\Delta\varepsilon^{e}_{im}) \tag{36}$$

Subtracting Eq. (35) from Eq. (36) and neglecting small terms of second order

$$\Delta\sigma_{im}=D^{im}\Delta\varepsilon^{e}_{im}+\Delta D^{im}\Delta\varepsilon^{e}_{im} \tag{37}$$

Considering assumption 5 and Eq. (33), ΔD^{im} may be expressed as follows.

where,

$$\Delta D^{im}=\frac{dD^{im}}{d\varepsilon_{im}}\Delta\varepsilon_{im}=\frac{dD^{im}}{d\varepsilon_{im}}(\Delta\varepsilon^{e}_{im}+\Delta\varepsilon^{p}_{im})$$

Substituting, ΔD^{im} in Eq. (37),

$$\Delta\sigma_{im}=D^{im}\Delta\varepsilon^{e}_{im}+\frac{dD^{im}}{d\varepsilon_{im}}\varepsilon^{e}_{im}\Delta\varepsilon^{e}_{im}+\frac{dD^{im}}{d\varepsilon_{im}}\varepsilon^{e}_{im}\Delta\varepsilon^{p}_{im}$$

$D^{im}+(dD^{im}/d\varepsilon_{im})\varepsilon^{e}_{im}$ is D^{B} of Eq. (19). Therefore

$$\Delta\sigma_{im}=D^{B}\ \Delta\varepsilon^{e}_{im}+\frac{dD^{im}}{d\varepsilon_{im}}\varepsilon^{e}_{im}\ \Delta\varepsilon^{p}_{im} \tag{38}$$

In the above equation, $\Delta\varepsilon^{e}_{im}$ is responsible for the change of average stress ($\sigma_{av}=\sigma_{im}$) due to the change of the stress at yielded points at the edges. $\Delta\varepsilon^{p}_{im}$ is responsible for the change of average stress due to the change of the effective width of the plate (implicitly expressed in D^{im}).

2.8 Elastic-plastic stiffness matrix

Plastic nodes[5] are inserted at the checking points where the yield condition is satisfied. Using Eq. (38) and following the procedures of the plastic node method, an elastic-plastic stiffness matrix may be derived which is capable of representing the decrease of the carrying capacity at the post-ultimate strength state. This matrix is, however, unsymmetric. A symmetric stiffness matrix is preferred for the efficiency of computation. A symmetric elstic-plastic stiffness matrix may be developed by introducing the concept of strain hardening rate and to represent the change of plate effectiveness caused actually by large deflection not by the material since it is assumed elastic perfectly-plastic. A virtual strain hardening (softening) is assumed such as that, $\Delta\sigma_{im}$ which is actually caused by the change of plate effectiveness due to $\Delta\varepsilon^{p}_{im}$ is treated as an increment of stress caused by this virtual strain hardening due to $\Delta\varepsilon^{p}_{im}$.

2.8.1 Virtual equivalent strain hardening rate $H_{eq})_v$

In the following a virtual equivalent strain hardening rate $H_{eq})_v$ is evaluated.

As mentioned before $\Delta\varepsilon^{e}_{im}(=\Delta\varepsilon^{e}_{av})$ in Eq. (38) corresponds to the change of the stress in the yielded checking points whose the yield conditions are still satisfied, while $\Delta\varepsilon^{p}_{im}(=\Delta\varepsilon^{p}_{av})$ causes a change $\Delta\sigma_{im}$ $(=\Delta\sigma_{av})$ due to the change of the plate effectiveness. The change of plate effectiveness is replaced by a virtual strain hardening.

Therefore in evaluating $H_{av})_v$ only the last term of Eq. (38) needs to be considered. $\Delta\sigma_{im}$ may be written as

$$\Delta\sigma_{im}=\frac{dD^{im}}{d\varepsilon_{im}}\varepsilon^{e}_{im}\ \Delta\varepsilon^{p}_{im} \tag{39}$$

$$\Delta\sigma_{im}=D_0\ \Delta\varepsilon^{p}_{im} \tag{40}$$

where,

$$D_0=\frac{dD^{im}}{d\varepsilon_{im}}\varepsilon^{e}_{im}=\frac{\partial D^{im}}{\partial\sigma_{im}}\frac{d\sigma_{im}}{d\varepsilon_{im}}\varepsilon^{e}_{im}+\frac{\partial D^{im}}{\partial\varepsilon_{im}}\varepsilon^{e}_{im}$$

In **Fig. 6.** Eq. (38) is illustrated in the case of one dimensional stress state for simplicity. According to the conventional treatment of strain hardening, an increment of stress is expressed as follows

$$\left.\begin{aligned}\Delta\sigma&=E\ \Delta\varepsilon^{e}_{v}\\&=E^{T}\ \Delta\ \varepsilon_{v}\\&=H\Delta\varepsilon^{p}_{v}\end{aligned}\right\} \tag{41}$$

where, $\Delta\varepsilon_v=\Delta\varepsilon^{e}_{v}+\Delta\varepsilon^{p}_{v}$ (41.a)

Here $\Delta\varepsilon^{e}_{v}$ and $\Delta\varepsilon^{p}_{v}$ are defined as increments of virtual elastic and plastic strains and are different from $\Delta\varepsilon^{e}_{im}$ and $\Delta\varepsilon^{p}_{im}$ as shown in Fig. 6. Comparing Eq. (40) with the second of Eq. (41) and considering Fig. 6 $\Delta\ \varepsilon_v$, E and E^{T} may be expressed as follows.

$$\left.\begin{aligned}\Delta\varepsilon_v&=\Delta\ \varepsilon^{p}_{im},\\E&=D^{B},\ \text{and,}\\E^{T}&=D_0\end{aligned}\right\} \tag{42}$$

H may be calculated as

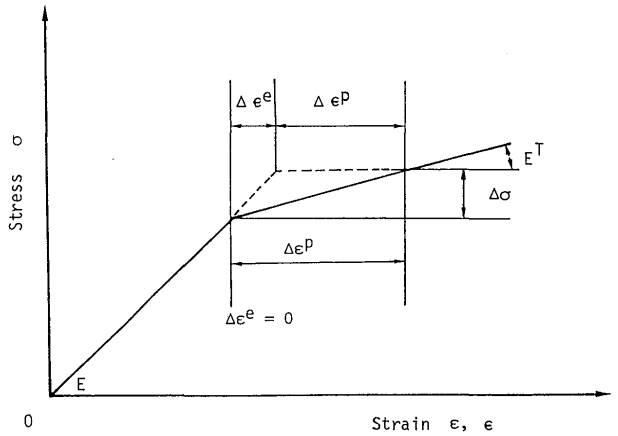

Fig. 6 One-dimensional stress strain relationship

$$H=([D_0]^{-1}-[D^{ep}]^{-1})^{-1} \tag{43}$$

The above relationships are expressed in terms of stress and strain. Similarly, the relation between the increments of nodal forces and nodal virtual plastic displacement (corresponding to virtual plastic strain) after yielding may be evaluated as follows.

$$\Delta R=K_0\ \Delta U^p_v \tag{44}$$

where, $K_0=\int B^T H B\ dv$ (45)

ΔU^p_v is an increment of virtual plastic displacement resulting from $\Delta\varepsilon^p_v$, the increment of virtual plastic strain.

As mentioned before, a plastic node is inserted at a checking point where yielding has started. The general expression of the plasticity condition at checking point i is given by the following equation[6].

$$F_i=\Gamma_{yi}(\sigma)-\sigma_{oi}=0 \tag{46}$$

where, $\Gamma_{yi}(\sigma)$ is the yield function. σ_{oi} is a function of the equivalent plastic strain ε'_{pi} and indicates the size of the yield surface at point i under yielding. The above equation may be written in terms of nodal force R as follows.

$$F_i=\Gamma_{yi}(R)-\sigma_{oi}=0 \tag{47}$$

The consistency condition may be written as

$$dF_i=0, \text{ that is } \{d\Gamma_{yi}/dR\}^T\ [dR]\ -d\sigma_{oi}=0 \tag{48}$$

Equating the external and the internal plastic works during a load increment.

$$\{R\}^T\{\Delta U^p_v\}=\int_v\sigma_{oi}d\varepsilon'_{pi}dv$$

Assuming that the plastic behaviour is the same over the whole plastic region i.e. $d\varepsilon'_{pi}$ is the same over the whole plastic region[6], then

$$\{R\}^T\{\Delta U^p_v\}=d\varepsilon'_{pi}\int_v\sigma_{oi}dv \tag{49}$$

According to the plastic node method,

$$\{\Delta U^p_v\}=\{d\Gamma_{yi}/dR\}d\lambda_i \tag{50}$$

Combining Eqs. (49) and (50), the following equation is obtained

$$d\varepsilon'_{pi}=c_i d\lambda_i \tag{51}$$

where, $c_i=\{R\}^T\{d\Gamma_{yi}/dR\}/\int_v\sigma_{oi}dv$

Substituting Eqs. (44), (50) and (51) into Eq. (48), the following quation may be obtained

$$(d\sigma_{oi}/d\varepsilon'_{pi})c_i d\lambda_i=\{d\Gamma_{yi}/dR\}^T[K_0]\ \{d\Gamma_{yi}/dR\}d\lambda_i \tag{52}$$

$(d\sigma_{oi}/d\varepsilon\varepsilon'_{pi})c_i$ is equal to $H_{eq})_{vi}$, the virtual equivalent strain hardening rate for the plate element at the yielded checking point i.

Therefore,

$$H_{eq})_{vi}=\{d\Gamma_{yi}/dR\}^T\ [K_0]\ \{d\Gamma_{yi}/dR\}$$

When the plasticity condition is satisfied at m nodes, the virtual equivalent strain hardening $H_{ar})_v$ may similarly be derived as follows

$$H_{eq})_v=[d\Gamma_y/dR]^T\ [K_0][d\Gamma_y/dR] \tag{53}$$

where, $[d\Gamma_y/dR]=[d\Gamma_{y1}/dR\ d\Gamma_{y2}/dR\ ....\ d\Gamma_{ym}/dR]$

2.8.2 Elastic-plastic stiffness matrix

When yielding occurs at node i, substitution of Eq. (51) into Eq. (48) produces

$$\{d\Gamma_{yi}/dR\}^T\ \{\Delta R\}=(d\sigma_{oi}/d\varepsilon'_{pi})c_1 d\lambda_i \tag{54}$$

or, $\{d\Gamma_{yi}/dR\}^T\ \{\Delta R\}=H_{eq})_{vi}d\lambda_i$

Putting $\{d\Gamma_{yi}/dR\}^T=\Phi_i{}^T$, and $H_{er})_{vi}=\Phi_i{}^T K_0\Phi_i$ into the above equation, it may be rewritten as

$$\Phi_i{}^T\Delta R=\Phi_i{}^T K_0\Phi_i d\lambda_i \tag{55}$$

Now ΔU, an increment of the total nodal displacement,

may be written as follows,

$$\Delta U=\Delta U^e+\Delta U^p \tag{56}$$

Here ΔU, ΔU^e and ΔU^p correspond to $\Delta\varepsilon_{im}$, ε^e_{im} and ε^p_{im}, respectively.

Considering the first of Eqs. (42) and (41.a),

$$\Delta U^p=\Delta U^e_v+\Delta U^p_v \tag{57}$$

where ΔU_v, ΔU^e_v and ΔU^p_v corespond to $\Delta\varepsilon_v$, ε^e_v and ε^p_v respectively.

Substituting Eq. (57) into Eq. (56), ΔU may be written as follows,

$$\Delta U=\Delta U^e+\Delta U^e_v+\Delta U^p_v$$

The increment of nodal forces may now be written as,

$$\Delta R=K^B(\Delta U^e_v+\Delta U^e)=K^B(\Delta U-\Delta U^p_v)$$

Substitutin Eq. (50) for ΔU^p_v then

$$\Delta R=K^B(\Delta U-\Phi_i d\lambda_i) \tag{58}$$

Substituting the above equation into Eq. (55), $d\lambda_i$ may be evaluated as,

$$d\lambda_i=\Phi_i{}^T K^B\ \Delta U/S_i \tag{59}$$

where, $S_i=\Phi_i{}^T(K^B+K_0)\Phi_i$ (59)

Substitution of Eq. (59) into (58) gives the increment ΔR of nodal force after yielding as follows,

$$\Delta R=K^p\Delta U$$

where K^p is the elastic-plastic stiffness matrix and is expressed as:

$$K^p=K^B-K^B\Phi_i\Phi_i{}^T K^B/S_i$$

When yielding occurs at m nodes, K^p may similarly be derived as follows,

$$K^p=K^B-K^B\Phi S^{-1}\Phi^T K^B \tag{60}$$

where, $\Phi=[\Phi_1,\Phi_2,\ .....,\ \Phi_m]$, $S=\Phi^T(K_0+K_0)\Phi$

3. Effect of initial deflection and residual stresses

As mentioned before, usually ship plates have initial deflection and residual stresses. These initial imperfections are produced at the fabrication processes, in particular due to welding. In this section, the effect of initial deflection and residual stresses on the behavior of plates is considered.

First, initial deflection is dealt. Initial deflection may be expressed in a fourier series as follows[7].

$$w_o=\sum_{m=1}^{\infty} W_{om}(\sin\ m\ \pi x/a)\ \sin(\pi y/b) \tag{61}$$

A plate with initial deflection and subjected to biaxial compression exhibits an increase of deflection from the beginning of the loading process. At the beginning, the magnitudes of all fourier components of the initial deflection increase. Close to the critical buckling load, unless some other component has an extremely large magnitude, the magnitude of the component similar to the buckling mode of the corresponding perfect plate continue to increase at a higher rate, while the magnitudes of other components start to decrease. Strictly speaking, bifurcation at the critical load is not observed. The behavior is accompanied with the effect of large deflection from the beginning of loading. Yielding starts at a load lower than that for a perfectly flat plate (without initial deflection) and ultimate strength is also reduced. Only one component of initial deflection similar to the buckling mode has an appreciable effect on plate behavior and needs to be taken into account. Initial deflection may then be expressed as follows.

$$w_o=W_{om}\sin(m\pi x/a)\ \sin(\pi y/b) \tag{62}$$

where, W_{om}=the amplitude of a component of initial deflection similar to the buckling mode,

m=the number of half buckling waves of the buckling mode.

The value of W_{om} to be used in design is given in Ref. 4) when average measured values are not available. The value of m depends on the plate aspect ratio and the ratio of $\sigma_{yav}/\sigma_{xav}$. It is the smallest integer satisfying the following equation.

$$\frac{(m^2b^2/a^2+1)^2}{m^2b^2/a^2+(\sigma_{yav}/\sigma_{xav})}\leqq\frac{\{(m+1)^2b^2/a^2+1\}^2}{(m+1)^2b^2/a^2+(\sigma_{yav}/\sigma_{xav})}$$

Initial deflection does not have a large effect on plate behavior in shear and in the case where the plate is subjected to shear stress together with biaxial compression, initial deflection may still be represented by Eq. (62).

Additional deflection due to the applied load may be assumed in the same form as follows.

$$w=W\sin(m\pi x/a)\ \sin(\pi y/b) \tag{63}$$

where, W is the amplitude of the additional deflection

Next, welding residual stresses are dealt. These usually take the distribution as in **Fig. 7-a** and may be idealized as in **Fig. 7-b**. This distribution is characterized by two tension bands near the edges where the stress reaches the yield stress, and a compressive region in the middle portion of the breadth of the plate. This stress distribution is in self-equilibrium. The effect of residual stress is directly related to the magnitude σ_r of the compressive region.

The effect of these residual stresses is to reduce the buckling load, the load at which first yielding occurs, as well as the ultimate strength and post-ultimate strength carrying capacity.

In the present formulation, when evaluating the large deflection behavior of the plate, effective compressive residual stresses distributed uniformly in x and y directions are assumed as follows[4].

$$\left.\begin{aligned}\sigma_{rex}&=\sigma_{rx}(1-.5\ \sigma_{rx}/(\sigma_{rx}+\sigma_o))\\ \sigma_{rey}&=\sigma_{ry}(1-.5\ \sigma_{ry}/(\sigma_{ry}+\sigma_o))\end{aligned}\right\} \quad (64)$$

where, σ_{rx} and σ_{ry} are magnitudes of the compressive residual stresses in x and y directions, respectively.

As mentioned above, the deflection of a plate with such imperfections, when subjected to external loads, starts to increase from the beginning of the loading process and the bifurcation at buckling is unclear. The behavior of such a plate may be treated in the same way as the post-buckling behavior of perfectly flat plates. In the following, the elastic stiffness matrix, ultimate strength condition and the post-ultimate strength elastic-plastic stiffness matrix are evaluated.

3.1 Elastic stiffness matrix

As being introduced in the evaluation of the post buckling stiffness matrix of a perfectly flat plate, a similar imaginary flat plate is employed, using the linear displacement functions of Eq. (8). Stress distributions are linear in this imaginary plate and the material properties are determined so that the plate exhibits similar stiffness to that of the deformed plate. Under loading, shortening in x and y directions and shear strain of the deflected plate may be evaluated, and the relation between average strain and average stress may be written as follows.

$$\left.\begin{aligned}\varepsilon_{xav}&=(\sigma_{xmax}^{*}-\nu\sigma_{yav})/E\\ \varepsilon_{yav}&=(\sigma_{ymax}^{*}-\nu\sigma_{xav})/E\\ \gamma_{xyav}&=\tau_{xy}/G_e\end{aligned}\right\} \quad (65)$$

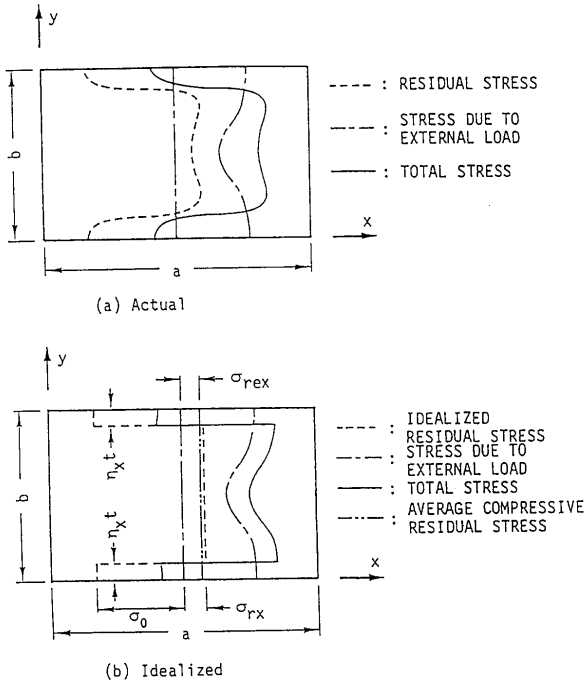

Fig. 7 Longitudinal stress distribution in a welded plate subjected to uniaxial compression

where, σ_{xav}, and σ_{yav} are the average stresses and σ_{xmax}^{*} and σ_{ymax}^{*} are the maximum membrane stresses caused by the external load. In order to determine the maximum membrane stresses, σ_{xmax}^{*} and σ_{ymax}^{*}, Galerkins method is applied to solve the equilibrium and compatibility equations of the plate[4]. σ_{xmax}^{*} and σ_{yav}^{*} are obtained as follows.

$$\left.\begin{aligned}\sigma_{xmax}^{*}&=\sigma_{xav}+1.62\sigma_{xcr}V^{2.4}+\sigma_{xL}\ (f_v+1)\\ \sigma_{ymax}^{*}&=\sigma_{yav}+1.62\sigma_{ycr}V^{2.4}+\sigma_{yL}\ (g_v+1)\end{aligned}\right\} \quad (66)$$

where, stress due to large deflection, σ_{xL} and σ_{yL}, are given by.

$$\sigma_{xL}=(0.125m\pi^2/a^2)EW(W+2W_{om})$$
$$\sigma_{yL}=(0.125\pi^2/b^2)EW(W+2W_{om})$$

and W can be calculated from the following equation,

$$C_1W^3+C_2W^2+C_3W+C_4=0$$

where, $C_1=E\left(\dfrac{m^4\pi^2}{a^4}+\dfrac{\pi^2}{b^4}\right)$, $C_2=3W_{om}C_1$

$$C_3=2W_{om}^2C_1+\frac{4\pi^2Et}{3(1-\nu^2)}\left(\frac{m^2}{a^2}+\frac{1}{b^2}\right)^2-16\left\{\frac{m^2}{a^2}(\sigma_{xav}+\sigma_{rex})+\frac{1}{b^2}(\sigma_{yav}+\sigma_{rey})\right\}$$

$$C_4=-16\left\{\frac{m^2}{a^2}(\sigma_{xav}+\sigma_{rex})+\frac{1}{b^2}(\sigma_{yav}+\sigma_{rey})\right\}W_{om}$$

Substituting maximum stresses σ_{xmax}^* and σ_{ymax}^* in Eq. (66) into Eq. (65) the relation between the average stress and the average strain may be obtained as follows.

$$\left.\begin{aligned}\sigma_{xav}&=\frac{1}{1-\nu^2}\left\{(E-\frac{F+H+\nu(F^*+H^*)}{\varepsilon_{xav}})\varepsilon_{xav}+\nu\ E\varepsilon_{yav}\right\}\\ \sigma_{yav}&=\frac{1}{1-\nu^2}\left\{\nu\ E\varepsilon_{xav}+(E-\frac{\nu(F+H)+F^*+H^*}{\varepsilon_{yav}})\varepsilon_{yav}\right\}\\ \tau_{xy}&=G_e\gamma_{xy}\end{aligned}\right\} \quad (67)$$

where, $F=\sigma_{xcr}(1.62\nu^{2.4})$ $\quad F^*=\sigma_{ycr}(1.62\nu^{2.4})$

$H=\sigma_{xL}\ (f_v+1)$ $\quad H^*=\sigma_{yL}\ (g_v+1)$

Now, replacing $\{\sigma_{av}\}$ and $\{\varepsilon_{av}\}$ in Eq. (67) by $\{\sigma_{im}\}$ and $\{\varepsilon_{im}\}$ respectively. The stress-strain relationship of the imaginary plate may be written as follows.

$$\sigma_{im}=D^{im}\varepsilon_{im} \quad (68)$$

where,

$$D^{im}=\frac{1}{1-\nu^2}\begin{bmatrix}(E-\frac{F+H+\nu(F^*+H^*)}{\varepsilon_{xim}}) & E\nu & 0\\ E\nu & (E-\frac{\nu(F+H)+F^*+H^*}{\varepsilon_{yim}}) & 0\\ 0 & 0 & (1-\nu)G_e\end{bmatrix}$$

Similar to the case of the perfectly flat plate, the increment of $\Delta\varepsilon_{im}$ due to an increment of $\Delta\varepsilon_{im}$ may be expressed by the following equation.

$$\Delta\sigma_{im}=D\Delta\varepsilon_{im}+\frac{\partial D^{im}}{\partial\sigma_{im}}\varepsilon_{im}\frac{d\sigma_{im}}{d\varepsilon_{im}}\Delta\varepsilon_{im}+\frac{\partial D^{im}}{\partial\varepsilon_{im}}\varepsilon_{im}\Delta\varepsilon_{im}$$

i.e., $\Delta\sigma_{im}=D^{B}\ \Delta\varepsilon_{im}$ (69)

where, $D^{B}=(I-\frac{\partial D^{im}}{\partial\sigma_{im}}\varepsilon_{im})^{-1}\ (D^{im}+\frac{\partial D^{im}}{\partial\varepsilon_{im}}\varepsilon_{im})$

and the post-buckling stiffness matrix is given as follows:

$$K^{B}=\int B^{T}D^{B}B\ dv \quad (70)$$

3.2 Ultimate strength condition

In presence of residual stresses, tension bands as shown in Fig. 7 exist along the edges. The widths of these tension bnads, ξ_x and ξ_y, may be expressed as follows.

$$\xi_x=0.5\sigma_{rx}b/(\sigma_o+\sigma_{rx})$$
$$\xi_y=0.5\sigma_{ry}a/(\sigma_o+\sigma_{ry})$$

Therefore, initial yielding may start just on the inside of these tension bands rather than outer edges.

As in the case of the flat plate element, the stresses due to external load, σ_x at $y=0$ and b, σ_y at $x=0$ and a, and τ_{xy} may be expressed as follows.

$$\sigma=S_2R$$
$$S_2=D^{p1}BK^{-1},$$
$$\text{and, } D^{p1}=E_e\begin{bmatrix}1 & \nu a_e/a & 0\\ \nu b_e/b & 1 & 0\\ 0 & 0 & G_e/E_e\end{bmatrix}$$

where, $E_e=E/[1-(b_ea_e/ba)\ \nu^2]$, b_e and a_e are the effective widths of plate element in the directions of x and y, respectively,

$$b_e/b=\sigma_{xav}/\sigma_{xmax}^*$$
$$a_e/a=\sigma_{yav}/\sigma_{ymax}^*$$

σ_x at $x=0$ and a, and $y=b/2$ may be evaluated as follows,

$$\sigma_x=\sigma_{xav}(1-\alpha_{xmin})=D_1^{im}BK^{-1}R(1-\alpha_{xmin})$$
$$\alpha_{xmin}=1.3(\sigma_{xcr}/\sigma_{xav})\nu^{2.1}+(\sigma_{xL}/\sigma_{xav})(0.3\nu+1)$$

σ_y at $y=0$and b in the middle of half buckling waves ($x=l/2$) may be evaluated as follows.

$$\sigma_y=\sigma_{yav}(1-\alpha_{ymin})=D_2^{im}BK^{-1}R(1-\alpha_{ymin})$$

where, $\alpha_{ymin}=1.3(\sigma_{ycr}/\sigma_{yav})\nu^{2.1}+(\sigma_{xL}/\sigma_{yav})(0.3\nu+1)$

For examination of initial yielding, stresses at the inside of the tension bands of residual stresses may be obtained as the sum of the residual stresses and the maximum stresses

$$\left.\begin{aligned}\sigma_{xmax})_{y=b-\xi_x}&=1/2[\sigma_x)_{y=b}-\sigma_x)_{y=b/2}]\cos2\pi\xi_x/b+\\ &\quad 1/2[\sigma_x)_{y=b}+\sigma_x)_{y=b/2}]+\sigma_{rex}\\ \sigma_{xmax})_{y=\ \xi_x}&=1/2[\sigma_x)_{y=0}-\sigma_x)_{y=b/2}]\cos2\pi\xi_x/b+\\ &\quad 1/2[\sigma_x)_{y=0}+\sigma_x)_{y=b/2}]+\sigma_{rex}\\ \sigma_{ymax})_{x=a-\xi_y}&=1/2[\sigma_y)_{x=a}-\sigma_y)_{x=l/2}]\cos2\pi\xi_y/a+\\ &\quad 1/2[\sigma_y)_{x=a}+\sigma_y)_{x=l/2}]+\sigma_{rex}\\ \sigma_{ymax})_{x=\ \xi_x}&=1/2[\sigma_y)_{x=0}-\sigma_y)_{x=l/2}]\cos2\pi\xi_y/a+\\ &\quad 1/2[\sigma_y)_{x=0}+\sigma_y)_{x=l/2}]+\sigma_{rex}\end{aligned}\right\} \quad (71)$$

Yielding is assumed to start at any location when Mises yield condition is satisfied, that is

$$\Gamma_y=\sigma_x^2-\sigma_x\sigma_y+\sigma_y^2+\sigma_y^2+3\tau_{xy}^2-\sigma_o^2=0$$

Expressing these stresses in terms of the nodal forces, the yield condition may be rewritten as.

$\Gamma_y = \Gamma_y(R) = 0$

3.3 Elastic-plastic stiffness matrix

In a similar way as in the case of the flat plate element, plastic nodes are inserted where the yield condition is satisfied. Having D^{im} and D^B of Eqs. (68) and (69), the elastic plastic stiffness matrix K^p may be rewritten as follows.

$$K^p = K^B - K^B \Phi S^{-1} \Phi^T K^B$$

where, K^B and S^{-1} are given by Eqs. (70) and (59) respectively, and Φ equal to $\{d\Gamma_y/dR\}$

4. Verification of Accuracy of the Improved Element

The improved ISUM plate element was presented in this paper to predict the post-ultimate strength of plates under different olads. In order to check the capability of the element, a series of analyses have been carried out and comparisons with results of analyses by the Finite Element Method are made. Analysis models are simply supported square plates with typical slenderness ratios of ship structural plates and different values of initial deflection. In the new element formulation, the effect of aspect ratio and residual stress on post-ultimate strength carrying capacity is assumed to be similar to their effect on ultimate strenght, which has been checked in Ref. 8). Therefore no checks on theses effects are performed here.

In the analysis by ISUM, each plate is modeled by one element . In the Finite Element Method analyses, models are composed of 10×10 to 16×16 elements (5×5 to 8×8 elements for one quarter of the plate) with 6 layers for evaluation of plasticity.

4.1 Uniaxial compression

Eleven simply supported squared plates as shown in **Table 1** are subjected to uniaxial compression in x-direction. The load is applied as a uniform displacement of the edge $x=a$, while keeping the edge $x=0$ stationary. The two edges $y=0$ and $y=b$ are free to move, however they are kept straight (ISUM plate element formulation guarantee straight edges). **Figures 8, 9** and **10** show results of analysis using the improved ISUM plate element together with those by FEM. It may be seen that this ISUM element predicts the decrease of the carrying capacity at the post-ultimate strength state. Results are generally in good agreement with results of the analysis by FEM. However, the following may be observed.

a. Since gradual progress of plasticity is not taken into account in the ISUM elements, a knuckle on p-Δ curve at the ultimate strenght may be observed. This leads to

Table 1 Geometrical and material properties of rectangular plates subjected to uniaxial compression loads

case	σ_y kgf/m²	a×b×t (mms)	λ	W_0/t	Fig. No.
1	28	1000×1000×16	2.28	0.01	8
2				0.1	
3				0.2	
4				0.5	
5	28	500×500×9	2.03	0.01	9-a , 9-b
6				0.25	
7				0.5	
8	28	1000×1000×24	1.52	0.01	10
9				0.1	
10				0.2	
11				0.5	

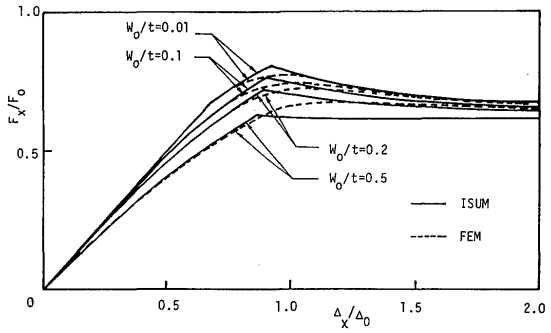

Fig. 8 Load-shortening relationships of uniaxially compressed square plates (cases 1, 2, 3 and 4, $\lambda=2.28$)

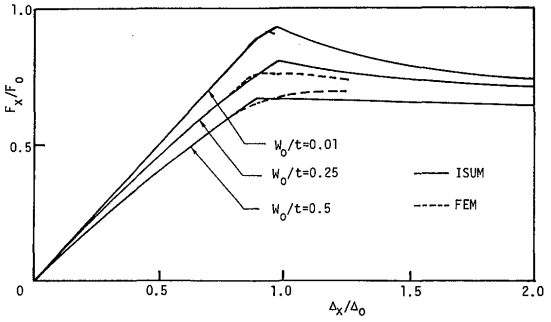

Fig. 9-a Load-shortening relationships of uniaxially compressed square plates (cases 5, 6,and 7, $\lambda=2.03$)

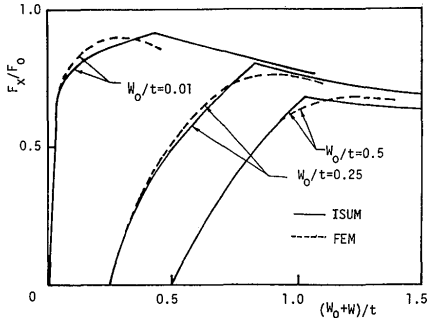

Fig. 9-b Load-deflection relationships of uniaxially compressed square plates (cases 5, 6,and 7, $\lambda=2.03$)

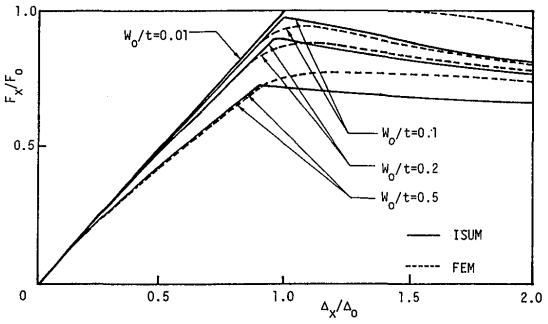

Fig. 10 Load-shortening relationships of uniaxially compressed square plates (cases 8, 9, 10 and 11, $\lambda=1.52$)

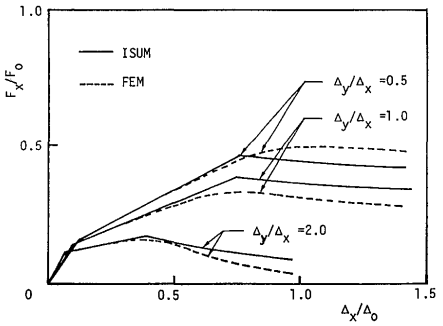

Fig. 11-a Load-shortening relationships of biaxially compressed square plates (cases 12, 13,and 14, $\lambda=3.65$)

a slight over-evaluation of the ultimate strength. As displacement increases, the carrying capacity quickly approaches that evaluated by the FEM.

b. With larger values of W_o/t, the ISUM element tends to slightly under-evaluate the ultimate strength, and post-ultimate strength carrying capacity.

4.2 Biaxial compressions

The analyses are performed on simply supported plates with $W_o/t=0.01$ under biaxial compressions, as shown in **Table 2**. The load is applied as unifor displacements Δ_x and Δ_y at the edges $x=a$ and $y=b$ respectively, while keeping edges $x=0$ and $y=0$ stationary. The loads with different ratios of Δ_y/Δ_x are applied. However, in each anaylsis, Δ_y/Δ_x is kept constant in the whole course of the analysis.

Figures 11 and **12** show results of the analyses by ISUM and by FEM. In Figs. 11-a and 12-a the non-dimensionalized relationship of the total force F_x in x-direction to the shortening Δ_x are plotted for plate thick-

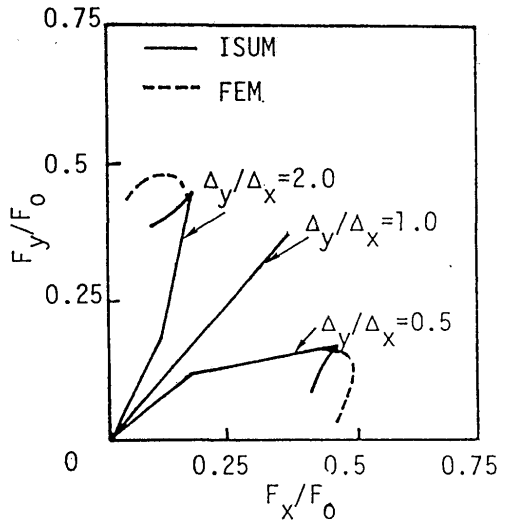

Fig. 11-b Ratio of compressive forces in x and y direction (cases 12, 13 and 14, $\lambda=3.65$)

Table 2 Geometrical and material properties of rectangular plates subjected to combined in-plane compression and shear loads.

case	σ_y kgf/m²	a×b×t (mms)	λ	W_0/t	load	Δ_y/Δ_x or $\Delta\varepsilon_x/\Delta_{xy}$	Fig. No.
12				0.01		0.5	11-a
13	28	1000×1000×10	3.65	0.01	$\sigma_x+\sigma_y$	1.0	11-b
14				0.01		2.0	
15				0.01		0.5	12-a
16	28	1000×1000×16	2.28	0.01	$\sigma_x+\sigma_y$	1.0	12-b
17				0.01		2.0	
18	28	1000×1000×6.7	5.45	0.01		—	
19	25	1000×1000×8.33	4.14	0.6	τ_{xy}	—	13
20	28	1000×1000×13.5	2.7	0.01		—	
21	28	1000×1000×16	2.28	0.01		1.0	
22	28	1000×1000×12	3.04	0.01		1.0	14-a
23	28	1000×1000×10	3.65	0.01	$\sigma_x+\tau_{xy}$	1.0	
24	28	1000×1000×12	3.04	0.01		0.666	
25	28	1000×1000×6	6.08	0.01		0.666	15-b

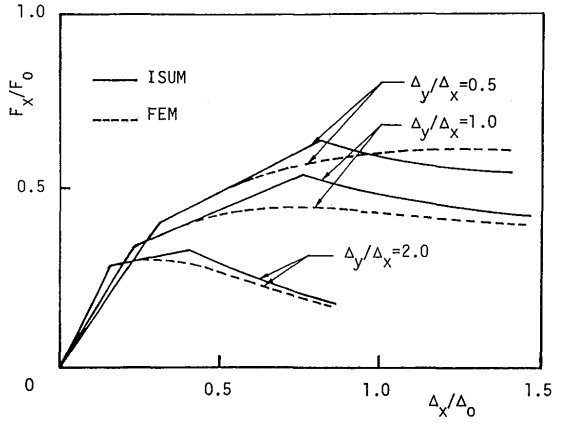

Fig. 12-a Load-shortening relationships of biaxially compressed square plates (cases 15, 16,and 17, $\lambda=2.28$)

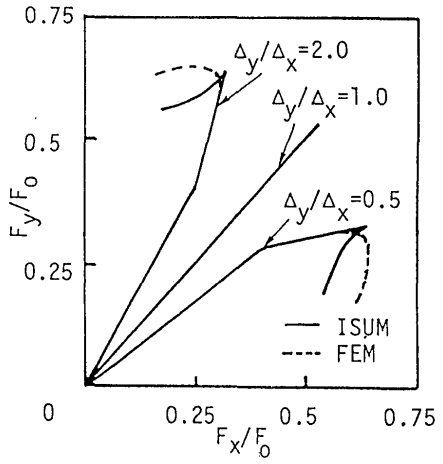

Fig. 12-b Ratio of compressive forces in x and y direction (cases 15, 16 and 17, $\lambda=2.28$)

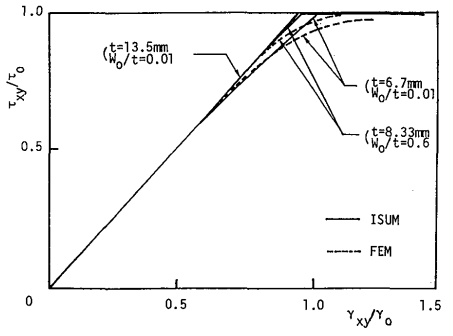

Fig. 13 Relationships of shear stress to shear strain of square plates subjected to pure shear (casses 18, 19 and 20)

nesses 10 and 16 mm. respectively and for different ratios of Δ_y/Δ_x. In the loading case where $\Delta_y/\Delta_x=0.5$ and 2, some difference between the results may be observed. This is in fact due to the loading method. Although the load is applied as forced displacement Δ_x and Δ_y with a constant ratio in both analyses, the tangential stiffnesses as evaluated by ISUM and FEM are different in the vicinity of the ultimate strength. This causes different ratio of the total forces F_x and F_y in x and y directions as shown in Figs. 11-b and 12-b. Loading with constant ratios of F_y/F_x would yield better agreement.

4.2 In-plane shear

Under in-plane shear, three simply supported square plates as shown in Table 2 are analysed. The load is applied in the form of imposed displacements, keeping all edges straight. By this loading condition, it is intended to produce only in-plane shearing forces. However, small values of in-plane axial forces could not be avoided in the FEM analyses. **Figure 13** shows the stress-strain relationships of these plates. Good agreements between results of ISUM and FEM may be observed. In all cases, the ultimate strength is equal or almost equal to the fully plastic strength. Post-ultimate strength carrying capacity is almost

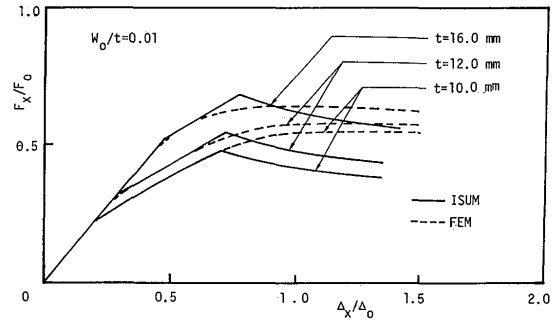

Fig. 14-a Load-shortening relationships of square plates subjected to uniaxial compression and shear (cases 21, 22 and 23)

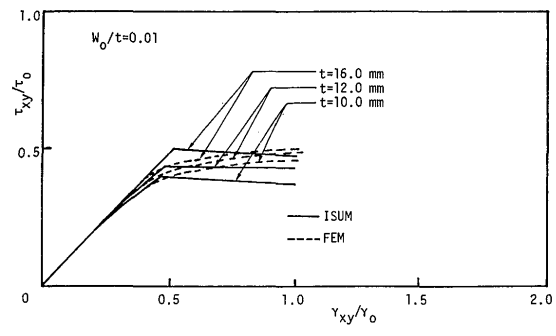

Fig. 14-b Relationships of shear stress to shear strain of square plates subjected to uniaxial compression and shear (cases 21, 22 and 23)

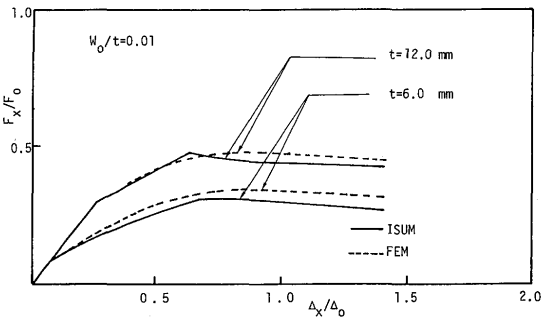

Fig. 15-a Load-shortening relationships of square plates subjected to uniaxial compression and shear (cases 24 and 25)

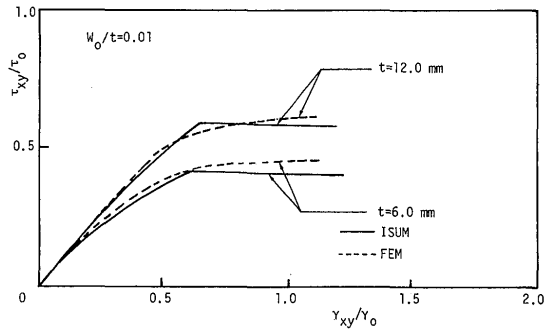

Fig. 15-b Relationships of shear stress to shear strain of square plates subjected to uniaxial compression and shear (cases 24 and 25)

constant, because the plate edges are kept straight.

4.4 Combined uniaxial compression and shear

The analyses are performed on simpley supported square plates with $W_o/t=0.01$ under combined in-plane uniaxial compression and shear loads, as shown in Table 2. In the analyses load is applied in each case as imposed displacement increments of a constant average strain ratio $\Delta\varepsilon_x/\Delta\gamma_{xy}$ at the edges $x=0$ and $x=a$ while keeping the edge $y=0$ statinary and the edge $y=b$ constrained in y-direction. **Figures 14-a** and **15-a** show load-shortening relationships of these plates. For the cases with a ratio of $\Delta\varepsilon_x/\Delta\gamma_{xy}=1.0$ ISUM predicts carrying capacity in the post-ultimate strength range lower than that predicted by the Finite Element Method. In the cases with $\Delta\varepsilon_x/\Delta\gamma_{xy}$ equal to 0.666 good agreement may be observed. Shear stress-shear strain relationships are shown in **Figs. 14-b** and **15-b**.

5. Conclusions

A new improved ISUM plate element is developed with the purpose of predicting reduction of the carrying capacity after ultimate strength has been reached. The new element can be used under in-plane uniaxial and biaxial compressions, bending and shear, and initial deflection and residual welding stresses can be taken into account.

Comparisons of results of the analysis using this improved element with results of the analysis by the Finite Element Method show generally good agreement. This new element would predict of ultimate strength and post-ultimate strength carrying capacity of redundant plate structures more accurately than the previous element.

Acknowledgment

This research is supported by Ministry of Education, Science and Culture, through the Grand-in-Aid for scientific research.

References

1) Ueda, Y. and Rashed, S. M. H., "The idealized Structural Unit Method and Its Application on Deep Girder Structures", Computer and Structures, Vol. 18, 1984.

2) Rashed, S. M. H.,"An Ultimate Transverse Strength Analysis of Ship Structures, The Idealized Structural Unit Method", Dr. Dissertation, Osaka University, Japan, 1975.

3) Ueda, Y., Rashed, S. M. H. and Paik, J. K., "Plate and Stiffened Plate Units of The Idealized Structural Unit Method (1st report)", J1 of Soc. of Naval Architecture of Japan, Vol. 156, 1984 (in Japanese).

4) Ueda, Y., Rashed, S. M. H. and Paik, J. K., "Plate and Stiffened Plate Units of The Idealized Structural Unit Method (2nd report)", J1 of Soc. of Naval Architecture of Japan, Vol. 159, 1986 (in Japanese).

5) Ueda, Y. and Yao, T., "The Plastic Node Method: A New Method of Plastic Analysis", J1 of Computer Methods in Applied Mechanics and Engineering, Vol. 34, No. 1-3, 1982.

6) Ueda, Y. and Fujikubo, M., "Generalization of The Plastic Node Method", J1 of Computer Methods in Applied Mechanics and Engineering, Vol. 92, 1991, pp. 33-35.

7) Ueda, Y. and Yao, T., "The Influence of Initial Deflection upon Compressive Ultimate Strength of Long Rectangular Plates", Transaction of JWRI, Vol. 13, No. 1, 1984.

8) Paik, J. K. "Ultimate Strength Analysis of Ship Structures by Idealized Structural Unit Method", Dr. Dissertation, Osaka University, Japan, 1987.

9) I. E. Harding, R. E. Hobbs and B. G. Neal, "Ultimate Load Behavior of Plates under In-Plane Loading, in Steel Plated Structures", Crosby Lockwood Staples, London, 1977.